공학석사 학위논문

Electrochemical LiOH Recovery from Used CO_2 Adsorbents

사용된 이산화탄소 흡착제로부터 전기화학적 LiOH 회수 연구

2019 년 8 월

서울대학교 대학원

화학생물공학부

최 민 준

Electrochemical LiOH Recovery from Used CO_2 Adsorbent

Minjune Choi

Chemical Convergence for Energy & Environment

School of Chemical and Biological Engineering

Seoul National University

Today the growing interests in indoor air quality caused the needs to control the indoor CO_2 concentration. Lithium hydroxide was one of the most widely used CO_2 capturing adsorbent material for its relatively large CO_2 uptake capacity and fast kinetics. However, the used Li-based CO_2 adsorbents were discarded, which caused the production of chemical wastes, and adsorbent recycling technologies had not been fully developed yet, even though the rapid increase in lithium compound risked the economically feasibility of the related industries.

In this study, the LiOH was recovered from the used CO_2 adsorbent via electrochemical method to develop an environmentally benign adsorbent recycling technology and maximize the feasibility of the electrochemical LiOH recovery system. By using electrocatalytic water splitting electrodes separated by a cation

exchange membrane, Li^+ were selectively recovered from O_2 evolving feed chamber to H_2 evolving recovery chamber. The effects of operating current to the electrochemical LiOH recovery system were studied and LiOH product was enriched up to 2.31M by consecutive cycle operations. Finally, the concentrated LiOH solution was crystallized to evaluate the energy required to produce 1g of LiOH powder which resulted in 28.1Wh/g_{LiOH}. The study on the effects of operation current to the electrochemical LiOH production system and the its corresponding energy evaluation will significantly affect the electrochemical adsorbent recycling technology and development of the environment friendly technology.

Keyword: Electrochemical lithium recovery, Electrodialysis, Lithium hydroxide, CO_2 adsorbent

Student number: 2017-20743

Contents

List of Figures

List of Tables

Chapter 1. Introduction

Air pollution has been considered as one of the most significant problems for humanity for the last several decades, and lately, interest in indoor air quality has been on a steep rise [1,2]. In particular, the concentration of carbon dioxide (CO_2) has drawn significant attention because it has significant impacts on human health. According to the US Occupational Safety and Health Administration, the standard of allowable indoor CO_2 concentration is 5000 ppm [3]; however, even 1000 to 2000 ppm of CO_2 makes people drowsy and may cause headaches, which consequentially reduce efficiency and productivity of daily lives [3,4]. Therefore, in order to control the amount of indoor CO_2, the development of CO_2 adsorbents have been widely carried out [5–10]. Among various materials [6,8,10–12], lithium hydroxide (LiOH) is the most commonly used due to its large capacity and fast kinetics in capturing CO_2 [12,13]. For this reason, LiOH is currently applied as CO_2 adsorbents in advanced facilities such as spacecraft and submarine, and it is also used in rebreathers [14,15].

These days, nearly 5% of globally produced lithium compounds are being consumed in air treatment industries [16]. Meanwhile, there has been a rapid increase in the price of lithium within the last several years, because of the growing demands for lithium-ion batteries that are used in electric vehicles and mobile devices [16–19]. This also led to a substantial rise in the market price of LiOH, which increased 3.48 times over the last 5 years [20,21]; as a result, the economic feasibility of LiOH

in CO_2 adsorbents became significantly lower. Since then, lithium recovery from various lithium sources such as spent lithium-ion batteries and brine has widely been studied [16,22–25]. Meanwhile, though LiOH adsorbents are seldom regenerated after capturing CO_2, there was an appreciable attempt to recover LiOH from used adsorbents [26]. Kim recovered LiOH from Li_2CO_3 by a precipitation method, wherein $Ca(OH)_2$ was employed as a precipitant. This process led to the successful recovery of LiOH; however, because porous media and polymeric binders are often utilized in commercial CO_2 adsorbents to maximize their performance [13,27], additional steps for separation of LiOH is necessary. Furthermore, the generation of chemical waste ($CaCO_3$) was an additional disadvantage of the precipitation method.

In this study, an electrochemical process for LiOH recovery from used CO_2 adsorbents is proposed. By using an electrochemical system comprised of catalytic electrodes (Pt and IrO_2) for water electrolysis [28–30] separated by a cation exchange membrane (CEM), LiOH was produced by selective electrodialysis of lithium ions through CEM and the generation of hydroxide ions from hydrogen evolution reaction. This strategy had two distinct advantages: (i) LiOH could be obtained without impurities such as other components of the adsorbents like porous media and binders (due to physical separation by CEM), and (ii) the whole process was environmentally benign because the use of additional chemicals or production of chemical wastes could be avoided. Moreover, by the repetitive cycle operation of the electrochemical system, concentrated LiOH solution could be obtained, and this resulted in a significant drop in energy consumption for evaporation of the solvent, which is

unavoidable when producing solid-state LiOH. In addition to the demonstration of the advantages mentioned above, a profound discussion to understand the behaviors of the diverse chemical species in this electrochemical system was carried out.

Chapter 2. Literature Review

2.1. Materials for CO_2 adsorption

To control the CO_2 concentration in the air, adsorption technology is commonly utilized which uses the CO_2 selective adsorbent. In Table 1, some of the most commonly utilized CO_2 adsorbent materials are summarized with its adsorption capacity and the corresponding adsorption conditions. Metal Organic Framework (MOF) and zeolites have been widely researched and used for its large surface area, high capacity, and well organized pore structure. However, these materials require high CO_2 pressure to achieve such high CO_2 capacity [31]. Also, calcium based adsorbents such as CaO, $Ca(OH)_2$ have been used based on its well-known adsorption chemistry [8]. Similarly, lithium based adsorbents are being used for the CO_2 capturing system due to its relatively large capacity and fast kinetics at standard temperature and pressure condition [13,27]. The most common types of lithium based adsorbent are LiOH which reacts with CO_2 and changes its form to Li_2CO_3 [12]. NASA also used LiOH as a CO_2 adsorbent for many years to maintain the CO_2 level in the spacecraft [14]. LiOH as a CO_2 adsorbent has also been applied to the submarine [15] and rebreather industry. Not only the LiOH, lithium silicate and lithium oxide have also been studied as an effective CO_2 adsorbent for its advantages [32,33].

Table 1. Common CO_2 adsorbent materials and the corresponding adsorption conditions and capacity.

Category	**Material**	**CO_2 adsorption condition**	**CO_2 adsorption capacity**	**Ref.**
MOF	MOF-177 [$Zn_4O(BTB)_2$]	298 K, 35 bar	33.5 mmol/g	[6]
	Ni_2(pbmp)	303 K, 1 bar	2.5 mmol/g	[34]
	MOF-210	298 K, 50 atm	2400 mg/g	[5]
Zeolite	Zeolite 13X	298 K, 32 bar	7.37 mmol/g	[7]
	NaX	298 K, 1 atm	4.98 mmol/g	[35]
Alkali metal	$Ca(OH)_2$	723 K, 1 bar	9.5 mmol/g	[8]
	Li_4SiO_4	773 K, 1 bar	6.14 mmol/g	[33]
	LiOH	298K, 1 atm	4.51 mmol/g	[13]
Carbon	AC	298 K, 300 psi	8.5 mmol/g	[36]

2.2. Recycling lithium from CO_2 adsorbents

2.2.1. Needs for lithium recovery from CO_2 adsorbent

The value of lithium compound has rapidly increased owing to its increased demand in electronic vehicle and portable device industries [17,18,20]. Due to the scarcity of the lithium sources which is limited to several brine lakes and ores, it is important for countries that are not benefited from the lithium sources to develop a technology of recycling the lithium compound from the waste products. The most common secondary lithium source is the lithium ion battery [16,24]. There are several technologies reported regarding lithium recovery from spent lithium ion batteries. However, most of the current recycling technologies include acid leaching, precipitation, thermal evaporation that is environmentally not friendly and energy intensive [24]. In addition, lithium ion battery recycling rate is currently around 3% of total LIB in the market, which is promising because of the progressive usage and demand of LIB in the future [16,20,21]. Also, lithium extraction not only from brine lakes and ores, but also from seawater and waste water is recently being reported to pioneer the alternative lithium source [22,25,37,38]. In the same vein, because nearly 5% of total lithium compound is distributed in air treatment industries [16], the usage of Li-based adsorbent without recycling is economically not feasible and environmentally not friendly as well. In order to improve the productivity and prevent the negative impact on the environment, it is inevitable to develop the adsorbent recycling technology that has not been intensively studied so far.

2.2.2. Conventional technology for recycling Li-based CO_2 adsorbent

Adsorbent recycling technology is mainly comprised of precipitation and acid leaching. As shown in Figure 1, Kim proposed the LiOH recovery by precipitation and evaporative crystallization method [26]. The governing precipitation chemistry is shown below.

$$Li_2CO_3 + Ca(OH)_2 \rightarrow 2LiOH + CaCO_3 \downarrow$$

By mixing 20g of Li_2CO_3, 20g of $Ca(OH)_2$, and 2000g of distilled water at 90 °C for 3 hours, $CaCO_3$ was formed, and it filtered to separate out the LiOH solution that has pH of 14.3. As shown in Figure 2, the produced LiOH solution was evaporated and crystallized at 500 °C. By this way, spent adsorbent, Li_2CO_3, was reproduced as 99 $_{wt}$% purity LiOH via precipitation method using $Ca(OH)_2$ to precipitate out the $CaCO_3$ with a conversion rate of 95% and yield of 80%.

However, the previous research used pure Li_2CO_3 to produce LiOH, whereas, the surface modified adsorbent, LiOH coated onto the porous material to improve the contact area with the air, was used in this research which is inappropriate to be applied in precipitation method. In addition, precipitation method produces the chemical sludge such as $CaCO_3$ which causes the extra treatment process and secondary pollution if not well treated.

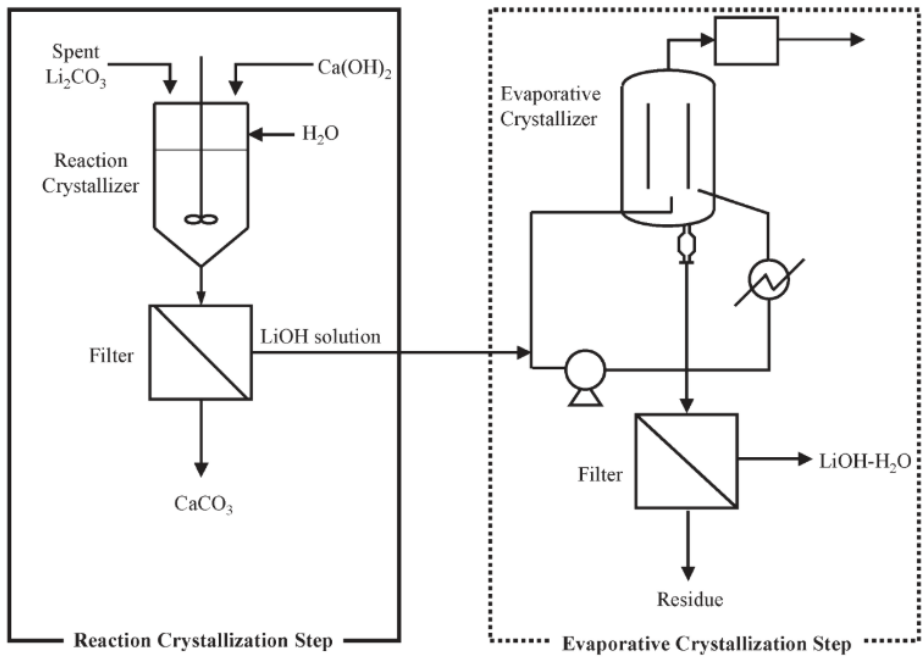

Figure 1. Overall process for lithium hydroxide recovery from spent lithium carbonate by evaporative crystallization technology [26].

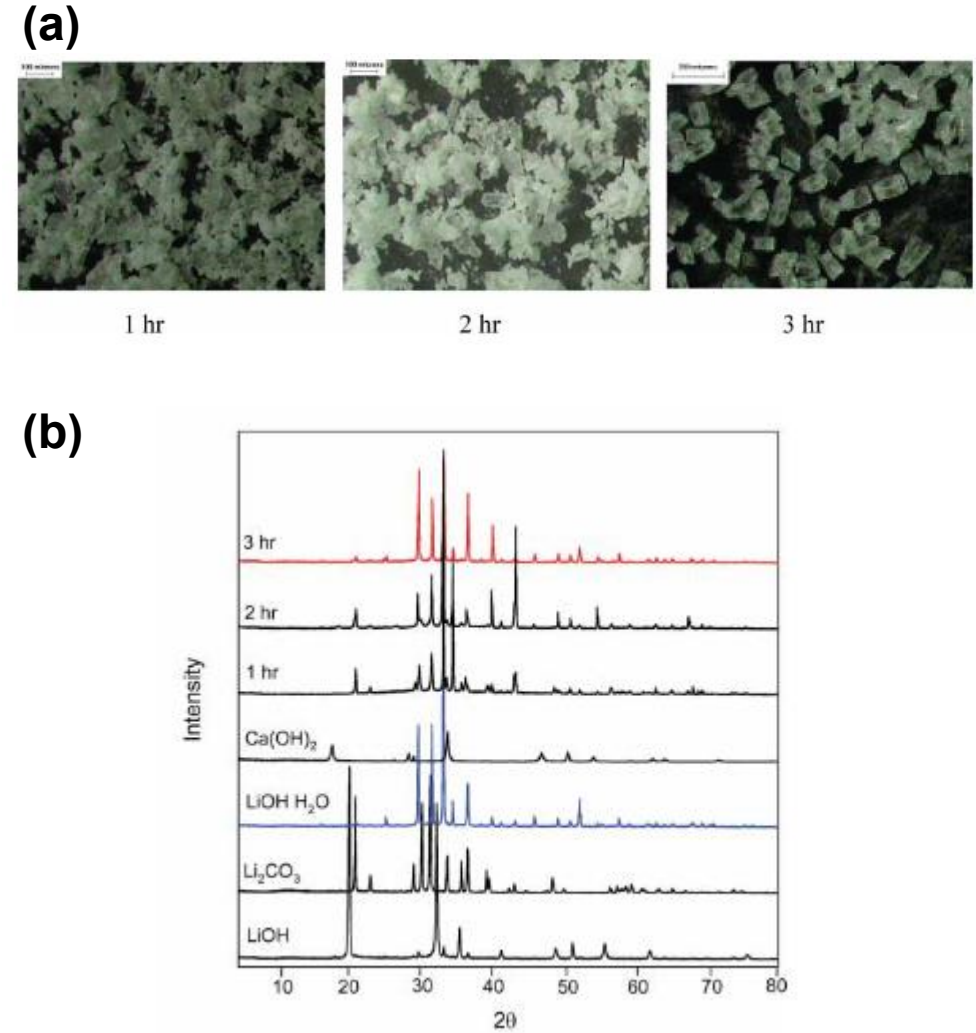

Figure 2. The LiOH recovered from spent Li_2CO_3 by evaporative crystallization. (a) SEM image of the crystallized LiOH with elapsed time and (b) XRD patterns of the produced LiOH differentiated by the evaporation time [26].

2.3. Electrochemical lithium recovery technologies

Electrochemical lithium recovery from spent LIBs requires aforementioned several pretreatment procedures before applying electricity [24,39–41]. After the pretreatment process that physically and chemically separates the impurities, the electrodialysis technology enables the recovery of lithium from the left over solution. Electrodialysis method is driven by the electrostatic force to separate and recover the target ions via cation exchange membrane [42–44]. It consumes less energy compared to the other technologies and more environmentally benign since electrodialysis neither requires chemical additives nor produces sludge unlike precipitation technology. The only energy applied in this method is the electrical energy which is economically advantageous when compared to the thermal evaporation or reverse osmosis [45]. Electrodialysis technologies have been commercialized in desalination process for more than 50 years. Separation of ions using electrodialysis has recently been deeply studied because even though the major cations in seawater is Na^+, the amount and the effect of Mg^{2+} is not negligible. In order to selectively separate Na^+ from Mg^{2+}, monovalent cation selective membrane is widely being utilized [46]. Therefore, these days electrodialysis is applied in various fields such as desalination [47], resource recovery [48,49], acid/base production [50–52], and heavy metal and nutritious chemical removal [42].

As shown in Figure 3, electodialysis is composed of four main parts; cathode, anode, ion exchange membrane, and electrolytes. When direct current is

applied to both electrodes, the electrical potential causes the water splitting reaction in the electrolyte. The water splitting reaction occurs in electrodialysis is shown below.

$$\text{Cathode:} \quad 4H_2O_{(l)} + 4e^- \rightarrow 2H_{2(g)} + 4OH^-_{(aq)}$$

$$\text{Anode:} \quad 2H_2O_{(l)} \rightarrow O_{2(g)} + 4H^+_{(aq)}\ 4e^-$$

Water molecule reacts with electron and splits into hydrogen and hydroxide ion in cathode, whereas, in anode, water molecule is oxidized and produces oxygen and electron. Due to the price competitiveness and easy H_2 generation availability, stainless steel is commonly used as the cathode material. In addition, dimensionally stable anode(DSA) such as IrO_2 and RuO_2, is commonly used as the anode material [43] and is being widely applied not only in electrodialysis, but also in electrochemical advanced oxidation process. In this study, by applying constant current to the system, water splitting reaction takes place in both electrodes, which causes charge imbalance in both aqueous electrolytes, and Li ions are transported through the cation exchange membrane to maintain the charge neutrality in the system.

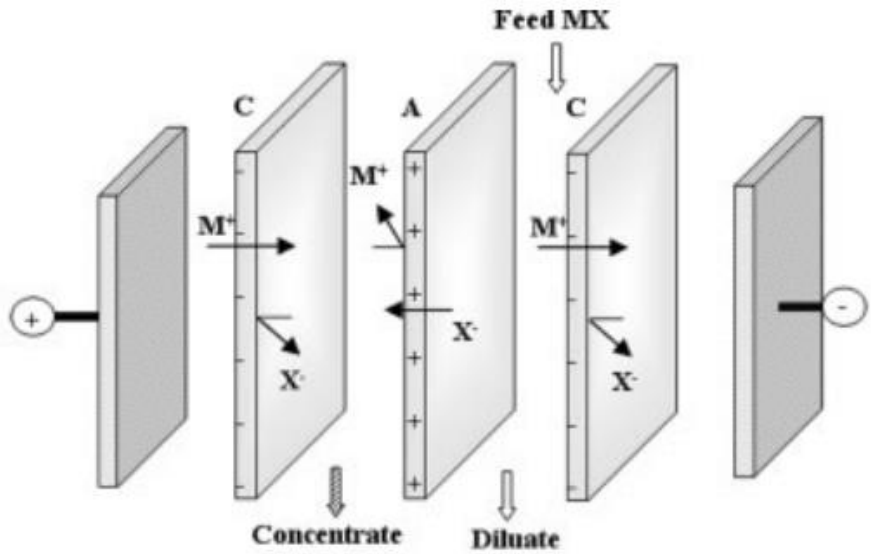

Figure 3. Schematics of electrodialysis process where M^+, X^-, C, and A represents cation, anion, cation exchange membrane, and anion exchange membrane, respectively [53].

Chapter 3. Materials and Method

3.1. Electrochemical LiOH recovery system

The CO_2 adsorbent used in this study was a commercialized product of Anytech Co. (Suwon, Republic of Korea), which was designed to capture CO_2 in subways. The used adsorbents were prepared by first putting the pristine adsorbents in a closed chamber and then flowing CO_2 gas into the chamber until concentrations of CO_2 at the inlet and outlet of the chamber became the same. As shown in Figure 4, in order to recover LiOH from used adsorbents, 2 g of ground CO_2 adsorbents were put into 40 mL of deionized water. The recovery chamber was filled with 40 mL of 10 mM LiOH at the beginning of each experiment. A platinum electrode (2.5×2.5 cm^2 mesh, Ametek) and IrO_2 electrode (2×3 cm^2 plate, Permelec Ltd.) were used as the anode and cathode respectively. Cation exchange membrane (CMD, Selemion) was placed between the feed solution and recovery solution. The system operation was carried out by applying the constant currents at room temperature using a battery cycler (WBC3000, WonAtech).

The LiOH enrichment process was operated by replacing feed solution (2 g of used adsorbent dissolved in 40mL of deionized water) under the same condition as before. One cycle in the LiOH enrichment process is defined as 2 hours of operation on electrochemical LiOH recovery from 2 g of used adsorbent. In order to

obtain LiOH, the solvent of recovery solution was evaporated at 120 ℃ for 30 min by using a vacuum oven (OV-11, JeioTech).

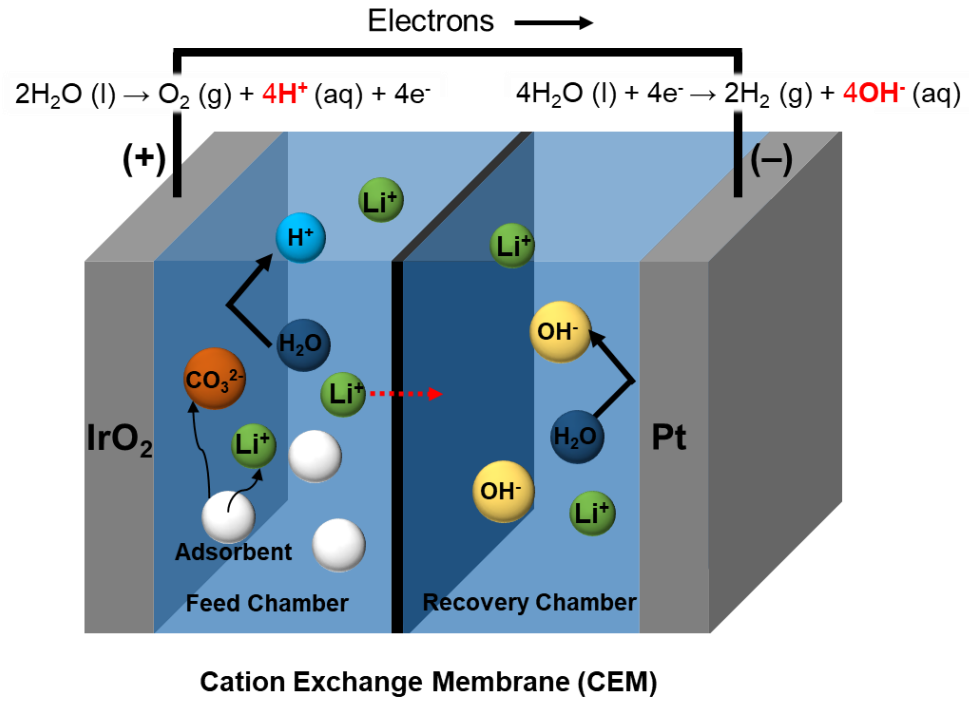

Figure 4. Schematic illustration of the electrochemical system for LiOH recovery from used CO_2 adsorbents.

3.2. Physicochemical characterizations

As shown in Figure 5, physical characterizations of CO_2 adsorbents and recovered LiOH were performed by scanning electron microscopy (SEM) and X-ray diffraction (XRD) by using Jeol JSM-7610 and Rigaku SmartLab, respectively. The content of lithium in CO_2 adsorbents was measured by Inductively Coupled Plasma (ICP) analysis using Shimadzu ICPS-8100 after acid leaching of the adsorbents. Lithium ion concentrations were measured by using an ion chromatography (ICS-1100, ThermoFisher, United States), after sampling 0.1 mL of solutions from feed and recovery chambers. The experiments were repeated three times to ensure the reliability of results.

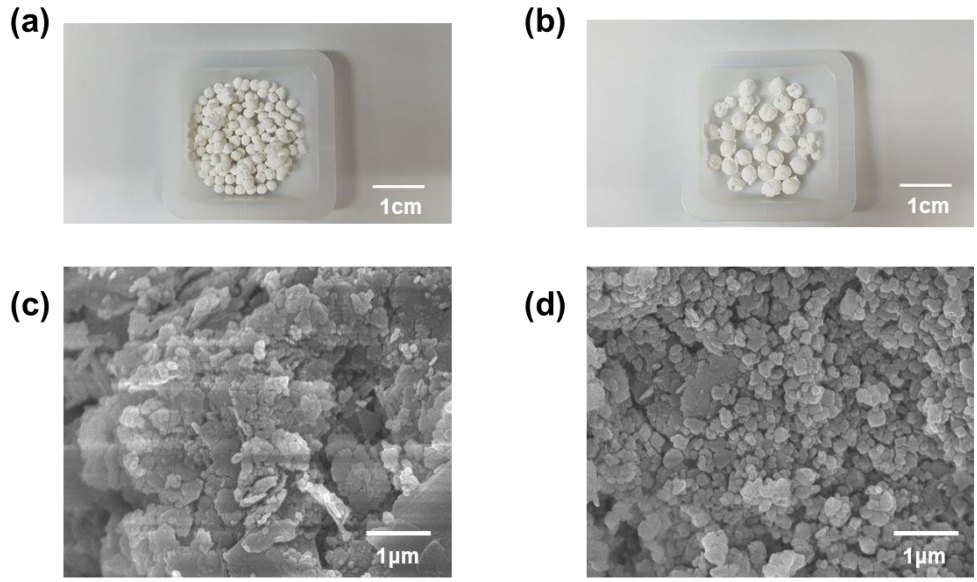

Figure 5. Physical characterizations of pristine and used CO_2 adsorbents. (a,b) Digital photograph and (c,d) SEM images of (a,c) pristine and (b,d) used CO_2 adsorbents.

3.3. Electrochemical LiOH recovery calculations

Recovery rate is the amount of Li ion transported from the feed solution to the final product solution during the electrochemical lithium ion recovery process. The feed adsorbent, however, contains substantial amount of impurities so, the mass fraction of the Li_2CO_3 in the used adsorbent was calculated for the accuracy.

$$Recovery\ rate = \frac{C_{f,Li}\ V\ M_{Li}}{m_{ads}\ x_{Li2CO3}\ y_{Li}} \times 100\%$$

where $C_{f,Li}$ is the final concentration of Li ion in the recovery chamber, V is the volume of the recovery chamber, M_{Li} is the molar mass of Li^+, m_{ads} is the mass of the used adsorbent, x_{Li2CO3} is the mass fraction of Li_2CO_3 within the adsorbent, and y_{Li} is the mass fraction of the Li^+ in Li_2CO_3.

Faradaic efficiency is the ratio of the amount of electrical charge used to transport the Li ion to the recovery chamber to the total electrical charge applied. It was calculated by the following equation.

$$Faradaic\ efficiency\ (\eta) = \frac{zF\Delta N}{It} \times 100\%$$

where z is the charge state of Li^+, F is Faraday's constant (96,485 C/mol), ΔN represents the amount of Li^+ transported, I is current, and t is total reaction time.

The energy required to produce LiOH via an electrodialysis method is calculated based on the equation shown below.

$$\mathrm{E} = \int V \cdot I \cdot dt$$

where V is the measured potential (V) and I is the applied current (A). The applied

current was constant in this system, so the measured voltage was integrated in terms of time, which gives the electrical energy required to produce LiOH from used CO_2 adsorbent.

Evaporation of the product requires heat energy which comprises the majority of the energy consumption. When calculating the heat energy (Q) consumed to evaporate water from the product solution so as to crystallize the LiOH, following equations were used with the consideration of boiling point elevation.

$$\Delta T_b = T_b - T_b^\circ = k_b \cdot m$$

$$Q = \int_{T_0}^{T_b} C_p^{liq} dT + \Delta H_{evap}$$

where T_b is the elevated boiling point of the solvent (ºC), T_b^o is the normal boiling point of the solvent (100 ºC), k_b stands for the ebullioscopic constant of water (0.52 ºC·kg/mol), m is the molality of the solution (mol/kg), C_p^{liq} is the specific heat capacity of water (4.1816 kJ/kg·K), and ΔH_{evap} is the enthalpy of vaporization of water (2,256.5 kJ/kg).

Chapter 4. Results and Discussion

4.1. Electrochemical LiOH recovery from used CO_2 adsorbents

4.1.1. Characterization of the CO_2 adsorbents

The morphology of the CO_2 adsorbent used in this study is shown in Figure 5. The adsorbent was comprised of LiOH, porous media, and organic binders and was in the form of granules, as depicted in Figure 5a. After the capturing CO_2, the size of granules increased to a larger extent, and this can be clearly seen from Figure 5b. In order to recover lithium from the used adsorbents and carry out further investigations, these adsorbents were ground into fine powders by using an agate mortar, to enhance the reliability of physical characterizations and facilitate the dissolution of adsorbent in further applications. Figure 5c and d show the SEM images of ground adsorbents before and after use, respectively.

Figure 6 shows the XRD patterns of the adsorbents. From the XRD measurement, it could be confirmed that the adsorbent, which is mainly LiOH at the pristine stage, turns into Li_2CO_3 after capturing CO_2. In order to measure the amount of lithium content in the adsorbents, ICP analysis was carried out, which revealed that there were 128.8 mg of lithium in 1 g of used adsorbents. Since the complete transition of LiOH to Li_2CO_3 during the CO_2 capture process (from the XRD patterns in Figure 6) was confirmed, it could be roughly assumed that all of Li in used

adsorbents exist in the form of Li_2CO_3, and this enabled the calculation of Li_2CO_3 content, which was 685.8 mg per 1 g of used CO_2 adsorbents.

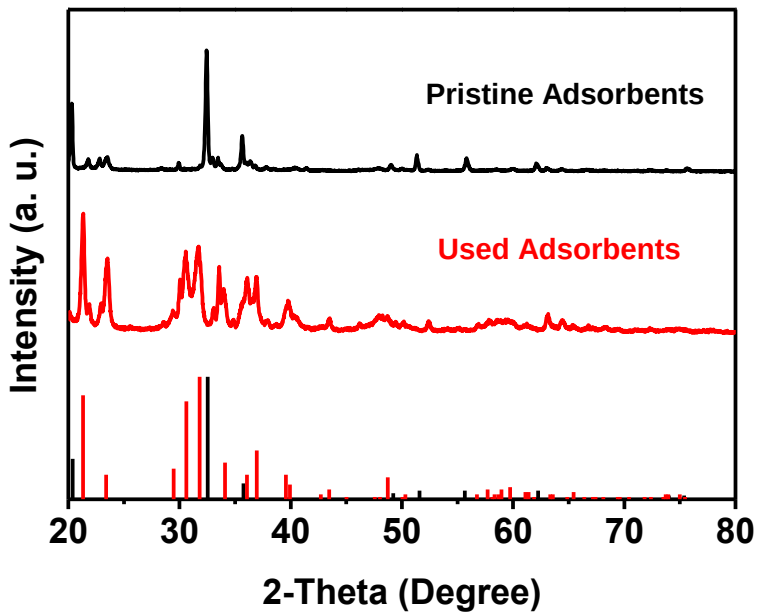

Figure 6. XRD patterns of pristine and used CO_2 adsorbents with reference peak positions for LiOH (JCPDS 01-1021, black bars) and Li_2CO_3 (JCPDS 22-1141, red bars).

4.1.2. Electrochemical LiOH recovery system

As described in Figure 4, the electrochemical system for LiOH recovery was a two-electrode cell separated by a CEM; oxygen-evolving IrO_2 electrode and feed solution were placed on one side (feed chamber), and hydrogen-evolving Pt electrode and recovery solution were placed on the other side (recovery chamber) of the CEM. In the compartment for feed solution, 2 g of adsorbents were dispersed in 40 mL of deionized water, and the solution was constantly stirred at 300 rpm. 10 mM LiOH solution was used as a recovery solution, in order to ensure sufficient ionic conductivity for reliable operation of the electrochemical cell. As the current was applied to the cell, the water splitting reaction took place, and protons and hydroxide ions were consequentially generated at IrO_2 and Pt electrodes, respectively. Then, in order to maintain the charge neutrality, Li^+ moved from the feed chamber to the recovery chamber, and as a result, LiOH concentration of the recovery chamber was increased, enabling the selective recovery of LiOH from the used CO_2 adsorbents.

4.1.3. Electrochemical LiOH recovery performances

The performances of the electrochemical lithium recovery system at various operation rates, by applying a diverse range of current; the operation current varied from 100 to 600 mA, with the cutoff cell voltage of 30 V were evaluated. Figure 7a shows the voltage profiles of the recovery system, and we could divide the stage of operations by different behaviors in the voltage profile. Regardless of the current, steep decrease in voltage was observed at the initial stage, followed by stabilization of voltage. The high voltage at the beginning could be attributed to significantly large membrane resistance, which decreases soon after being wetted by the system operation [54,55]. Meanwhile, the stabilized cell voltage was higher in the case of faster operations, because the overpotential for electrolysis reaction gets larger at higher current. After this stage, the voltage profiles showed the characteristic behaviors; they slightly increased and then decreased, before the rise of voltage at the end of the operation which is caused by depletion of Li^+ in the feed chamber. Figure 7b shows the voltage profile with regard to the applied charge. From the similar tendency of the profile, decent rate capability of our electrochemical system could be noted.

Figure 7c and d show the Li^+ concentration in feed and recovery solutions of the system, respectively. Initial feed solution contained 435 mM of Li^+ (0.64 g_{Li2CO3}), which is only 47% of total Li_2CO_3 in the feed solution; a significant portion of lithium was remaining in solid Li_2CO_3 before the system operation. This indicates that the

initial feed solution was saturated with Li^+, and this is roughly in line with the solubility of Li_2CO_3 in pure water at room temperature, which is 368 mM [56]. After starting the operation, the characteristic behaviors were observed from the Li^+ concentration profiles; slight drop and rise followed by a rapid decrease of Li^+ concentrations, regardless of the operation rates. Meanwhile, from the depletion of Li^+ in the feed solution after certain hours of operation and the linear increase of Li^+ concentration in the recovery chamber, we could verify that Li^+ could be recovered from the CO_2 adsorbents with high reliability.

Based on the concentration of recovery chamber, lithium recovery rate and speed were calculated with regard to the initial amount of present Li^+ and the time taken for the recovery, respectively which are summarized in Figure 8a. Given that the final concentration of Li^+ in recovery solutions were 784, 748, 707, and 694 mM when the operation currents were 100, 200, 400, and 600 mA, the recovery rate, the portions of Li_2CO_3 that was recovered as LiOH were 84.6, 80.73, 76.25, 74.49%, respectively. The smaller amount of LiOH was obtained when the system was operated at a faster rate, and this is ascribable to limited supply of lithium ions from adsorbents. On the other hand, the recovery speed, the amount of recovered LiOH divided by operation time, increased as the larger current was applied. From these experimental results, it could be deduced that the operation current should be carefully selected with the considerations on both recovery rate and recovery speed.

Figure 8b shows the Faradaic efficiency and energy consumption during the operation of electrochemical LiOH recovery process under various current condition.

Faradaic efficiency was higher at when the operation current was smaller, and this can also be understood as the consequence of sufficient lithium ion supply in the case of slower-rate operations. Meanwhile, as the applied current was varied from 100 to 600 mA, the energy consumption increased from 5.88 to 16.4 Wh/g_{LiOH}. Larger overpotential at higher current, which was observable from Figure 7b, seems to be the major reason for the increased energy consumption at faster operations.

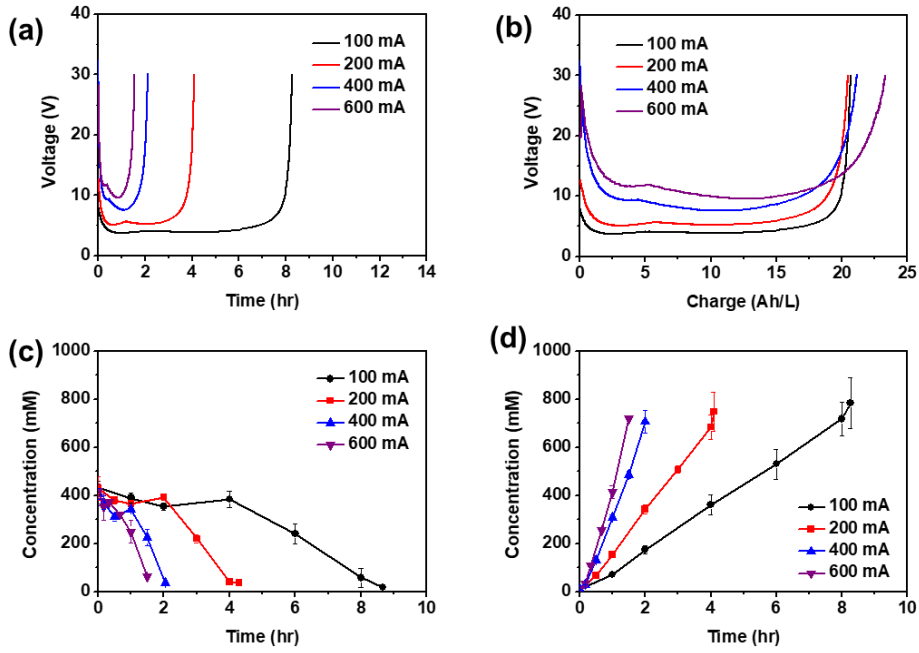

Figure 7. Electrochemical behaviors of the LiOH recovery system. (a,b) Voltage profiles at various operation currents presented with regard to (a) operation time and (b) applied charge. (c,d) Li^+ concentration profiles in (c) feed chamber and (d) recovery chamber.

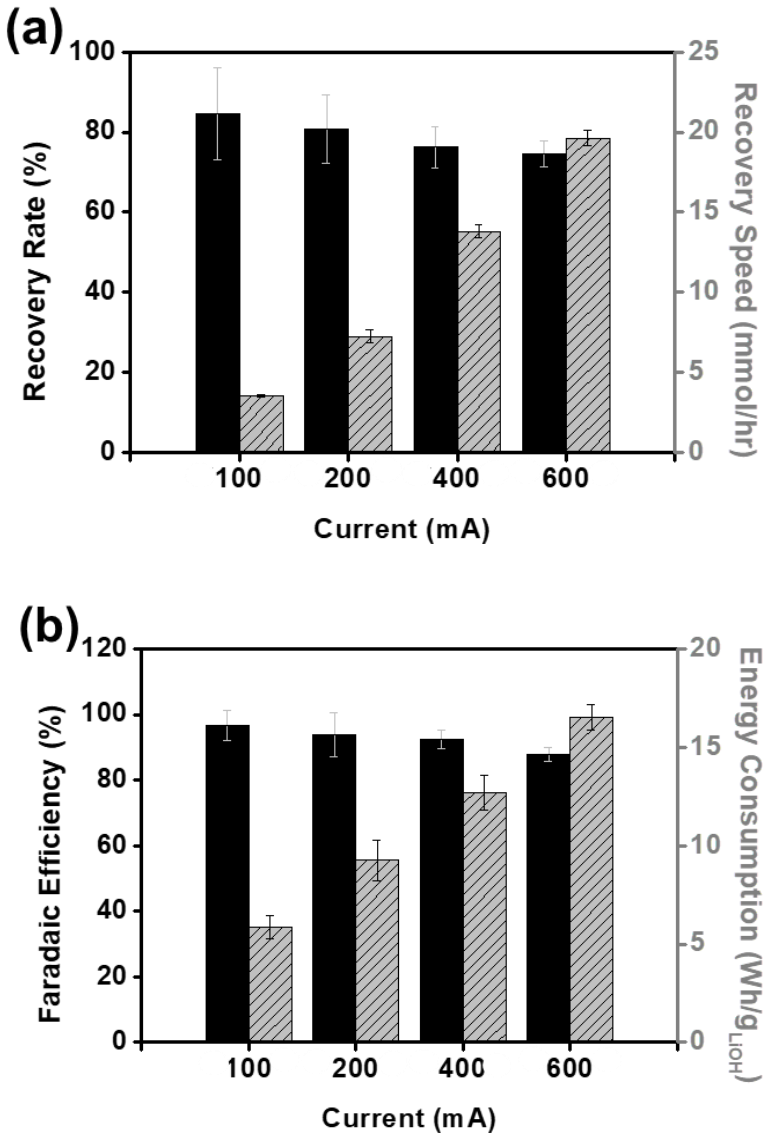

Figure 8. Electrochemical performances of the LiOH recovery system. (e) LiOH recovery rate (black bars) and recovery speed (grey bars) of the electrochemical system at diverse operation currents. (f) Faradaic efficiency (black bars) and energy consumption (grey bars) during the LiOH recovery.

4.2. Chemical phenomena in the LiOH recovery system

Though the feasibility of the system could be verified by experimental observations above, theoretical calculations were carried out to understand the behaviors of various chemical species within the electrochemical LiOH recovery system during the operation [57]. In order to simplify the calculation, several assumptions were made: (i) The system is always in equilibrium and the temperature remained constant, (ii) CEM completely blocks transfer of anions between feed chamber and recovery chamber, and (iii) the influences of the components in adsorbents other than Li_2CO_3 was neglected. Since Li_2CO_3 was put in the feed solution, the concentrations of lithium, carbonate, bicarbonate, carbonic acid, hydroxide ions, and proton were considered. To retain the charge neutrality in the feed chamber, the following equation must be satisfied:

$$[H^+] + [Li^+] = [OH^-] + 2[CO_3^{2-}] + [HCO_3^-] \quad (1)$$

In addition, because the system was assumed to be in equilibrium, following equilibrium constants should be satisfied.

$$K_w = [H^+][OH^-] = 10^{-14} \quad (2)$$

$$K_{a,1} = [H^+][HCO_3^-] / [H_2CO_3^*] = 10^{-6.3} \quad (3)$$

$$K_{a,2} = [H^+][CO_3^{2-}] / [HCO_3^-] = 10^{-10.3} \quad (4)$$

Considering that lithium and carbonate ions in the feed chamber solely originate from Li_2CO_3 in the adsorbents, the amount of Li^+ from the dissolution of Li_2CO_3 should be twice that of CO_3^{2-} and its derivatives; HCO_3^- and H_2CO_3*, while an asterisk was used to indicate both H_2CO_3 and its decomposed form ($H_2O + CO_2$). As noted in equations (3) and (4), carbonate ions and their derivatives in aqueous solution form carbonate buffer system, and the lowest pH value of the system during the LiOH recovery was 5.97 from the calculation based on the above equations. This indicates that proton concentration is kept low in this system. Since $[Li^+]$ is substantially larger than $[H^+]$ (by several degrees of orders) in the system while recovering LiOH, we could make an additional assumption that cation moving through the CEM (to adjust the charge balance) during the system operation is solely Li^+. Then, in the feed chamber, following equation is valid:

$$2([CO_3^{2-}] + [HCO_3^-] + [H_2CO_3^*]) = [Li^+] + (I \times t / FV) \quad (5)$$

where I is the applied current, t is the operation time, F is Faradaic constant, and V is the volume of feed chamber, and $I \times t / FV$ thereby represents the concentration of Li^+ in recovery chamber, which migrated from the feed chamber through the CEM.

Meanwhile, prior to the system operation, it was observed from the experimental results that significant portions of Li_2CO_3 is not dissolved in water. Until, the complete dissolution of Li_2CO_3, it can be regarded that Li_2CO_3 is saturated

in the feed chamber. Then, based on the assumption that the system is in equilibrium, following relationship on solubility product should be satisfied while solid Li_2CO_3 is remaining in the feed solution.

$$K_{sp} = [Li^+]^2[CO_3^{2-}] = 2.5 \times 10^{-2} \quad (6)$$

After all the Li_2CO_3 in the adsorbents are released in ionic states, the feed solution is no longer a saturated solution, and thereafter the concentration of Li^+ in feed chamber can be predicted by the following equation.

$$[Li^+] = 2N_{Li2CO3}/V - (I \times t / FV) \quad (7)$$

where N_{Li2CO3} is the total amount of Li_2CO_3 in the adsorbents.

Based on the above equations, the concentrations of each ion during the operation of the electrochemical LiOH recovery system were calculated, and the results are displayed in Figure 9a. As the oxygen evolution and generation of proton occur in feed chamber, Li^+ migrates to recovery chamber. Then, further dissolution takes place to satisfy the equation (6), until the moment of complete Li_2CO_3 dissolution at the applied charge value of 10.2 Ah/L by our calculation. When Li_2CO_3 dissolves into two Li^+ and one CO_3^{2-}, one Li^+ migrates to the recovery solution, and CO_3^{2-} forms HCO_3^- by reacting with H^+ (see equation (4)). As a result, due to the lowered Li^+ and CO_3^{2-} concentration in the feed chamber, the remaining

Li_2CO_3 further dissolves into the solution and at the same time, Li^+ accumulates in the feed chamber, which matches with the gradual increase in Li^+ concentration until 10.2Ah/L shown in Figure 9a. Since K_{sp} should be remained to the same value, CO_3^{2-}, which was initially presented in the feed chamber by spontaneous dissolution of Li_2CO_3 prior to the system operation, also gradually turns into HCO_3^-. This can be clearly observed from Fig. 4a, where a gradual decrease of CO_3^{2-} concentration and continuous increase in the amount of HCO_3^- occur during the operation before applying 10.2 Ah/L.

After the complete dissolution of Li_2CO_3 (i.e. applied charge exceeds 10.2 Ah/L), $[Li^+]$ decreases because Li^+ continues to migrate to recovery chamber while additional formation of Li^+ does not take place. Due to the same reason, the generation of CO_3^{2-} does not occur, and $[CO_3^{2-}]$ thereby shows a steeper drop until reaching close to zero. $[HCO_3^-]$ increases at the same rate until CO_3^{2-} is nearly used up, because protons generated by applying constant current react with CO_3^{2-} without any relevance to whether it was formed before or after the beginning of the LiOH recovery. Meanwhile, after $[CO_3^{2-}]$ becomes close to zero, H^+ generated at the anode reacts with HCO_3^- and forms H_2CO_3*.

On the other hand, regarding the changes in ion concentrations in recovery chamber, only $[H^+]$, $[OH^-]$, and $[Li^+]$ had to take into account. As water electrolysis occurs, the same amount of H^+ and OH^- get generated at anode and cathode, respectively, and also the same number of Li^+ migrates from feed chamber to recovery chamber to balance the charges. As a result, at constant current operation,

[Li^+] and [OH^-] linearly increase, as depicted in Figure 9b. This not only indicates that the system can be operated with precise control over the amount recovered LiOH. pH in recovery chamber during the system operation was calculated, and the effectiveness of the LiOH recovery system design could be supported by the increase in pH value, from 12 to 13.9.

In order to evaluate the reliability of the calculation, the experimentally measured [Li^+] and calculated values were compared for both feed chamber and recovery chamber, as displayed in Figure 10a and b, respectively. The trends of the changes in [Li^+] values obtained by theoretical and experimental procedures showed rough, but clear agreements, though there was some gap between them. Meanwhile, a notable mismatch was observed at the feed chamber during the initial stage of the operation; the experimental [Li^+] is significantly higher than the calculated results in this region. In the previous section, we mentioned that Li^+ concentration in feed solution is 435 mM before the current was applied; however, 368 mM is the theoretical maximum of [Li^+] at equilibrium, considering the solubility of Li_2CO_3. This discrepancy is likely attributed to our rough assumption that the components in adsorbents other than Li_2CO_3 do not have any effect on the system, because binders may get dispersed in water and change the chemical properties of feed solution and solubility of Li_2CO_3 in feed chamber. The amount of lithium larger than the known saturated concentration (368 mM) seems to result in the decrease of [Li^+] in the feed chamber at the initial stage (up to the applied charge of around 5 Ah/L), as the migration of Li^+ to the recovery chamber would be relatively more favored compared

to the generation of Li^+ by dissolution of Li_2CO_3, in order to meet the equilibrium in equation (6).

Meanwhile, after the initial stage, the trends in the change of [Li^+] obtained by theoretical calculation and experimental measurements matched well. In the feed chamber, after applying around 5 Ah/L of charge, [Li^+] increased linearly up to around 10 Ah/L, followed by linear decrease of [Li^+] with similar rates (slopes). In the recovery chamber, the changes in Li^+ concentration showed a high agreement with the calculation results. Considering that the theoretical and experimental values match well in recovery chamber during the whole operation, the influence of binder is also expected as the origin of the gap between theoretical and experimental values in the feed chamber even after the initial stage. In both chambers, the discrepancy between the theoretical and experimental results increased as the operation currents were increased, since the assumption that the system is always in equilibrium was made; time for the system to reach equilibrium state is less sufficiently given when the rate of system operation is faster. From the linearly increasing [Li^+] in the recovery chamber, regardless of the operation currents, the high reliability of our electrochemical system for LiOH recovery could be verified.

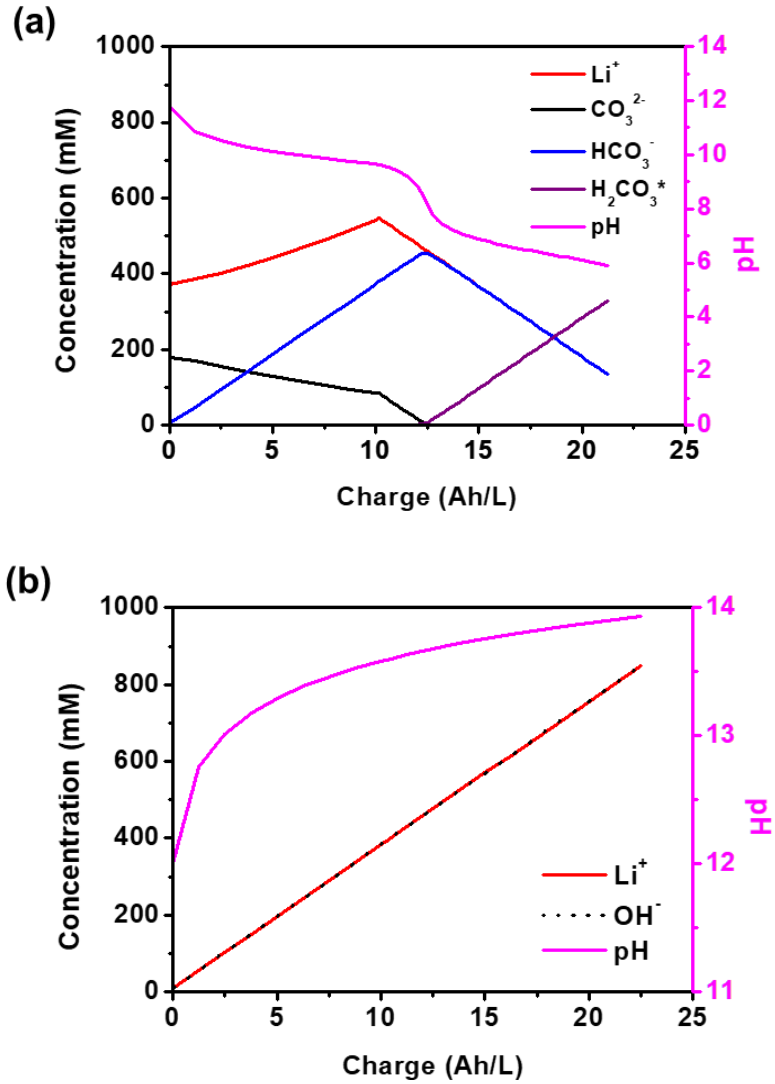

Figure 9. Calculated concentration profiles of active ion species in (a) feed chamber and (b) recovery chamber based on solubility product of Li_2CO_3, mass balance, and charge balance in aqueous system.

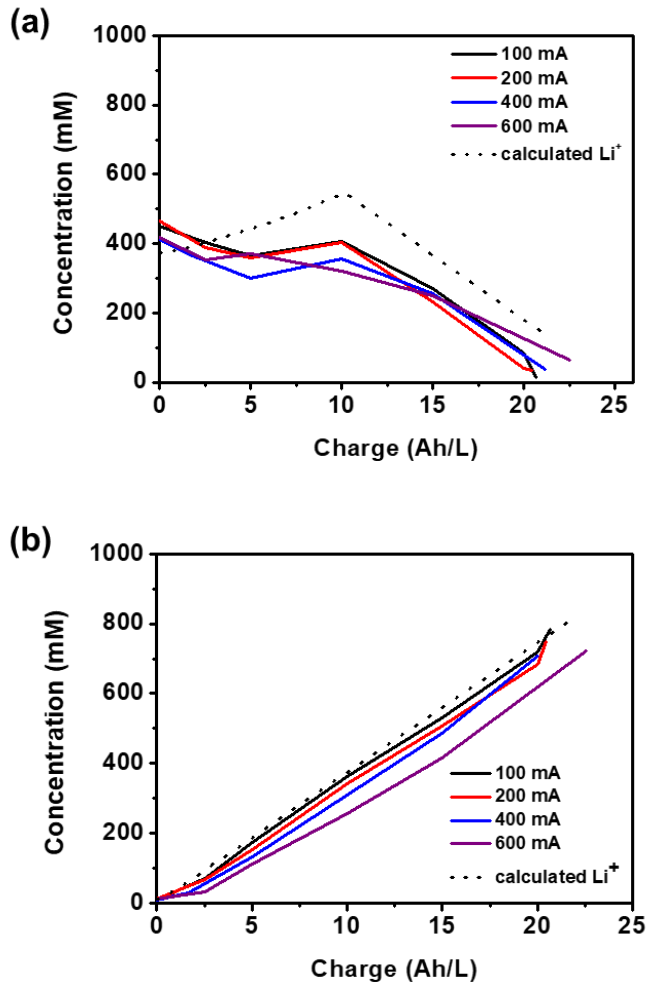

Figure 10. Comparison between Li^+ concentration profiles obtained from theoretical calculations and experimental measurements from Fig. 3. (c) and (d): in (c) feed chamber and (b) recovery chamber.

4.3. LiOH enrichment process to maximize feasibility

4.3.1. Electrochemical LiOH enrichment process

By using the electrochemical cell, LiOH solution was successfully obtained from the used CO_2 adsorbents; however, LiOH should be obtained in the form of powders to be reused in industry. Generally, the acquisition of LiOH powder from solution inevitably requires evaporation and crystallization processes [26], which necessitate large amounts of energy input [58]. Regarding the needs for minimizing energy consumption, increasing the concentration of LiOH in the recovery solution is expected to be highly favorable. In order to obtain a highly concentrated LiOH solution, the system was operated for 5 cycles, which in total for 10 hours. For each cycle, the electrochemical system was operated for 2 hours, and the solution in the feed chamber (which is used adsorbents dispersed in water) was replaced, while the recovery solution remained unchanged during the repetitive operation. Based on the experimental observations on rate capability (see Figure 10b), the system was operated at 400mA, because there was no significant drop in energy efficiency up to this current.

Figure 11a shows the voltage profile of the electrochemical LiOH recovery system during the consecutive operations in 5 cycle. At the initial stage of the first cycle, rapid drop in voltage was observable; from around 30 to 10 V. This voltage decay can be attributed to the wetting of CEM during the initial operation of the system, which results in a substantial decrease in membrane resistance. Then, there

was a further drop in voltage to 7.7 V at a milder rate, which seems to be resulted from the increased Li^+ concentration in feed chamber, which takes place until the complete dissolution of Li_2CO_3 in used adsorbents; the voltage then began to rise due to the decrease in [Li^+]. After replacing the feed solution after 2 h, the cell voltage was low because of the high initial Li^+ concentration, as discussed in the previous section. In addition, since the membrane was already wet owing to the previous cycle, membrane resistance was small from the beginning of the cycle. It was discussed above that [Li^+] undergoes a slight decrease and increase until the moment when all of Li_2CO_3 dissolved in the feed solution, followed by continuous drop until Li^+ is used up in the feed chamber. The voltage profile matched well with this explanation, and from the similar voltage profile in following cycles, feasibility of the electrochemical system in repetitive operation could be verified. During the consecutive operation, [Li^+] in the recovery chamber was measured, as depicted in Figure 11b. The concentration of Li^+ in the recovery solution linearly increased even after the repetitive replacements of feed solutions. From this observation, the effectiveness of the system was clearly verified, not only in LiOH recovery, but also in the enrichment of LiOH, which is important for the minimization of energy consumption in practical applications. After the 5 cycle, 2.31 M of LiOH solution was obtained, which means that the concentration of Li^+ increased by around 0.463 M per 2 g of adsorbents, which were replaced every 2 hours.

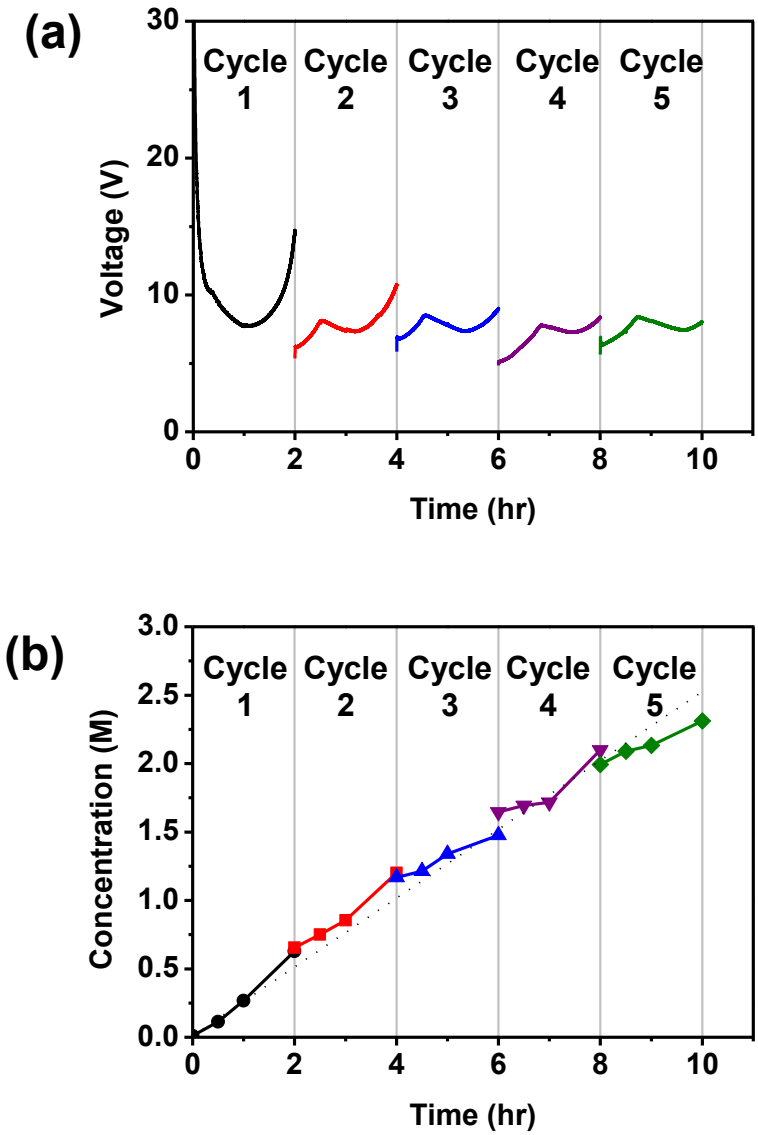

Figure 11. LiOH enrichment by consecutive cycle operations. (a) Voltage profiles and (b) Li^+ concentration profiles during 5 cycles which in total 10 hours of operation.

4.3.2. Energy consumption of the electrochemical LiOH recovery system

As mentioned in the previous paragraph, LiOH production, thermal evaporation should be accompanied by the electrochemical recovery process. Therefore, when calculating the total energy consumption to produce LiOH powder from used CO_2 adsorbents, the energy input for thermal evaporation should also be taken into account. Fig. 12 shows the total energy consumption with regard to the operation time, which is the sum of energies consumed for the operation of the electrochemical system and thermal evaporation. As shown in Figure 12, the total energy consumption was decreased as the operation time increased; though there was no significant increase in energy consumed for the electrodialysis, significant drop in energy consumption was achievable during the evaporation of solvents. In the case of consecutive cycle operations for 10 hours, total energy consumption was only 28.1 Wh/g_{LiOH}, which is less than 50% of that consumed during the LiOH recovery for 2 hours. Therefore, by concentrating LiOH by repetitive replacement of feed solution, LiOH can be recovered by using a substantially smaller amount of energy, increasing the overall economic feasibility of the system for practical and industrial applications.

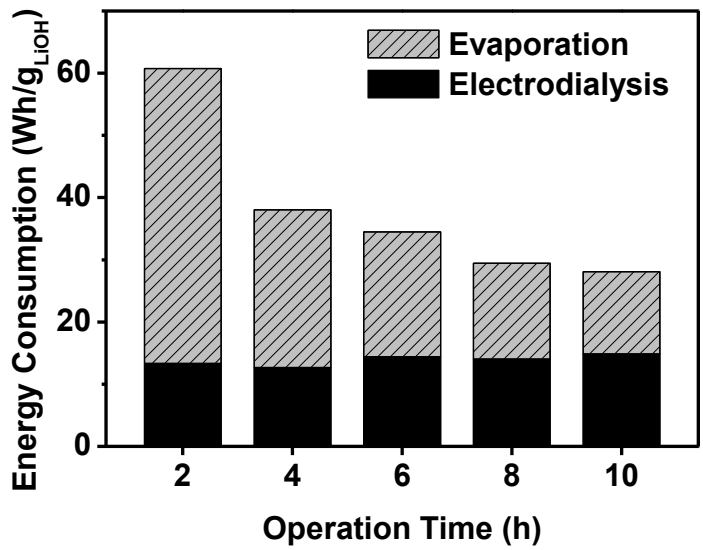

Figure 12. Estimated energy consumption for production of LiOH, which was calculated as the sum of the energies consumed for operation of the electrochemical recovery system and thermal evaporation of solvents.

4.3.3 LiOH product characterization

Additionally, characterizations on LiOH obtained by 10 hours of operation was carried out, first by titration of the recovery solution by using 5 M HCl. From the shape of the titration curve displayed in Figure 13, it could be verified that the recovery solution was strong base. This enabled the assumption that the amounts of components in the recovery solution other than LiOH is negligible, and the estimated concentration of LiOH is 2.45 M. Recovery of LiOH was corroborated by XRD analysis of the white powders obtained after evaporation of solvent (Figure 14a), and morphologies of recovered LiOH was characterized by SEM analysis (see Figure 14b).

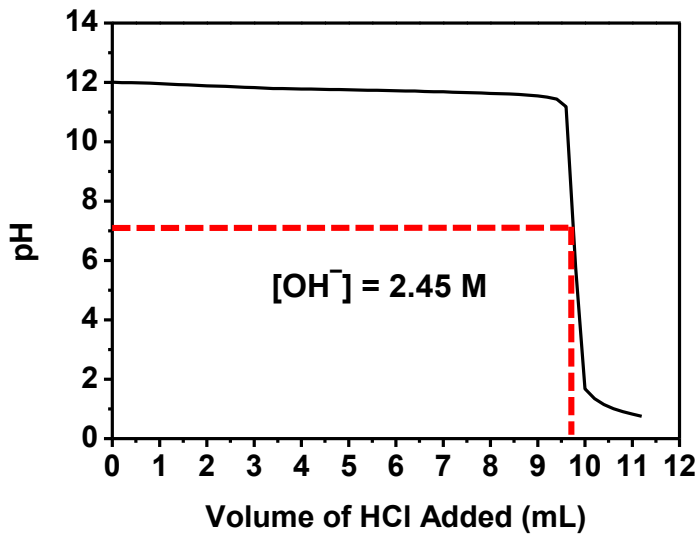

Figure 13. Titration graph of the concentrated LiOH solution obtained after 5 cycles of operation. 5 M of HCl solution was used for the titration

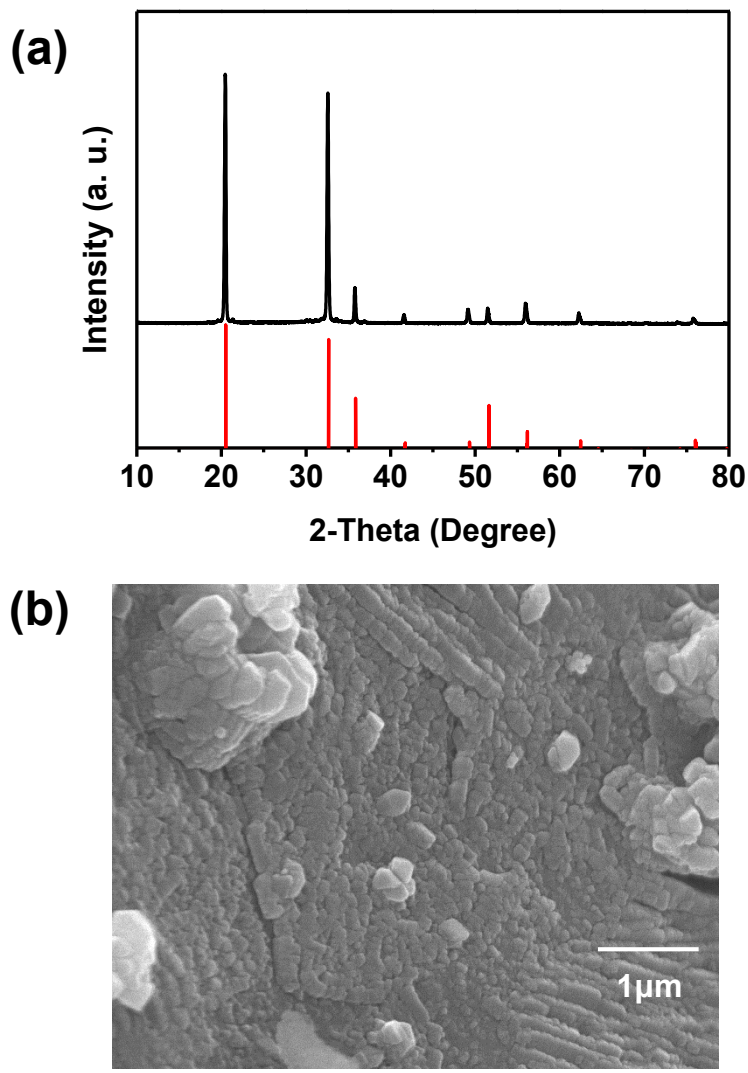

Figure 14. XRD pattern (a) and SEM image (b) of recovered LiOH after 5 cycles of operation; red bars in (a) shows the reference peak positions for LiOH (JCPDS 01-1021).

Chapter 5. Conclusions

In this study, LiOH was successfully recovered from the used CO_2 adsorbents using an electrochemical system which was comprised of electrocatalytic water splitting electrodes and a CEM. After investigating the influences of operating currents (100mA, 200mA, 400mA, 600mA) on the electrochemical LiOH recovery performances, lower operation currents were favored for the better recovery rate, energy consumption, and the faradaic efficiency, whereas, in terms of the recovery speed, faster operation currents were favored. In addition, the feasibility of the electrochemical LiOH recovery system was maximized by consecutive cycle operations of the system at 400mA operation current. The recovery solution was concentrated up to 2.31M of LiOH by consuming significantly reduced energy of 28.1Wh/g_{LiOH}, which is the half of the initial operation, mainly by decreasing the energy input for evaporation of solvents. Based on the simplicity, reliability, and environmentally benign characteristic, the electrochemical system proposed in this study is expected to be favorable for practical and industrial applications.

References

[1] T. Godish, Relationships between ventilation and indoor air quality: A review, Indoor Air. 6 (1996) 135–145.

[2] B.F. Yu, Z.B. Hu, M. Liu, H.L. Yang, Q.X. Kong, Y.H. Liu, Review of research on air-conditioning systems and indoor air quality control for human health, Int. J. Refrig. 32 (2009) 3–20.

[3] OSHA, Indoor Air Quality in Commercial and Institutional Buildings, 2011. https://www.osha.gov/Publications/3430indoor-air-quality-sm.pdf.

[4] S. Choi, J.H. Drese, C.W. Jones, Adsorbent materials for carbon dioxide capture from large anthropogenic point sources, ChemSusChem. 2 (2009) 796–854.

[5] H. Furukawa, N. Ko, Y.B. Go, N. Aratani, S.B. Choi, E. Choi, A.O. Yazaydin, R.Q. Snurr, M. O'Keeffe, J. Kim, O.M. Yaghi, Ultrahigh Porosity in Metal-Organic Frameworks, Science (80-.). 329 (2010) 424–428.

[6] A.R. Millward, O.M. Yaghi, Metal-organic frameworks with exceptionally high capacity for storage of carbon dioxide at room temperature, J. Am. Chem. Soc. 127 (2005) 17998–17999.

[7] S. Cavenati, C.A. Grande, A.E. Rodrigues, Adsorption Equilibrium of Methane, Carbon Dioxide, and Nitrogen on Zeolite 13X at High Pressures, J. Chem. Eng. Data. 49 (2004) 1095–1101.

[8] S.F. Wu, T.H. Beum, J.I. Yang, J.N. Kim, Properties of Ca-base CO2 sorbent using Ca(OH)2 as precursor, Ind. Eng. Chem. Res. 46 (2007) 7896–7899.

[9] D.M. D'Alessandro, B. Smit, J.R. Long, Carbon dioxide capture: Prospects for new materials, Angew. Chemie - Int. Ed. 49 (2010) 6058–6082.

[10] H. Yang, Z. Xu, M. Fan, R. Gupta, R.B. Slimane, A.E. Bland, I. Wright, Progress in carbon dioxide separation and capture: A review, J. Environ. Sci. 20 (2008) 14–27.

[11] M. Kato, K. Nakagawa, K. Essaki, Y. Maezawa, S. Takeda, R. Kogo, Y. Hagiwara, Novel CO2 absorbents using lithium-containing oxide, Int. J. Appl. Ceram. Technol. 2 (2005) 467–475.

[12] T.M. Tovar, M.D. LeVan, Supported lithium hydroxide for carbon dioxide adsorption in water-saturated environments, Adsorption. 23 (2017) 51–56.

[13] Y. Cho, J.Y. Lee, A.D. Bokare, S.B. Kwon, D.S. Park, W.S. Jung, J.S. Choi, Y.M. Yang, J.Y. Lee, W. Choi, LiOH-embedded zeolite for carbon dioxide capture under ambient conditions, J. Ind. Eng. Chem. 22 (2015) 350–356.

[14] S. Satyapal, T. Filburn, J. Trela, J. Strange, Performance and properties of a solid amine sorbent for carbon dioxide removal in space life support applications, Energy and Fuels. 15 (2001) 250–255.

[15] R.P. Dawkins, H.M. Gehrhardt, Efficient removal of carbon dioxide from an undersea habitat using adsorption techniques, Ocean Eng. 2 (1970) 27–31.

[16] B. Swain, Recovery and recycling of lithium: A review, Sep. Purif. Technol. 172 (2017) 388–403.

[17] M. Armand, J.-M. Tarascon, Building better batteries, Nature. 451 (2008) 652–657.

[18] S.K. Jung, H. Gwon, J. Hong, K.Y. Park, D.H. Seo, H. Kim, J. Hyun, W.

Yang, K. Kang, Understanding the degradation mechanisms of LiNi0.5Co0.2Mn0.3O2cathode material in lithium ion batteries, Adv. Energy Mater. 4 (2014) 1–7.

[19] H. Kim, J. Hong, K.Y. Park, H. Kim, S.W. Kim, K. Kang, Aqueous rechargeable Li and Na ion batteries, Chem. Rev. 114 (2014) 11788–11827.

[20] R. Baylis, Evaluating and forecasting the lithium market from a value perspective, in: 5th Lithium Supply Mark., 2013: pp. 1–29. http://www.indmin.com/events/download.ashx/document/speaker/6566/a0ID000000X0jbjMAB/Presentation.

[21] C. Werber, Global lithium prices, Quartz. (2016). https://qz.com/783314/this-is-what-electric-cars-are-doing-to-the-lithium-market/.

[22] S. Kim, J. Lee, J.S. Kang, K. Jo, S. Kim, Y.E. Sung, J. Yoon, Lithium recovery from brine using a λ-MnO2/activated carbon hybrid supercapacitor system, Chemosphere. 125 (2015) 50–56.

[23] A.H. Hamzaoui, A. M'nif, H. Hammi, R. Rokbani, Contribution to the lithium recovery from brine, Desalination. 158 (2003) 221–224.

[24] Y. Song, Z. Zhao, Separation and Puri fi cation Technology Recovery of lithium from spent lithium-ion batteries using precipitation and electrodialysis techniques, Sep. Purif. Technol. 206 (2018) 335–342.

[25] S. Kim, J. Kim, S. Kim, J. Lee, J. Yoon, Electrochemical lithium recovery and organic pollutant removal from industrial wastewater of a battery recycling plant, Environ. Sci. Water Res. Technol. 4 (2018) 175–182.

[26] K.J. Kim, Recovery of lithium hydroxide from spent lithium carbonate using crystallizations, Sep. Sci. Technol. 43 (2008) 420–430.

[27] Y.M. Cho, Y.M. Yang, D.S. Park, S.B. Kwon, W.S. Jung, J.Y. Lee, Study on CO2 Adsorption on LiOH-Modified Al2O3, Appl. Mech. Mater. 284–287 (2013) 342–346.

[28] O.H. Kim, Y.H. Cho, S.H. Kang, H.Y. Park, M. Kim, J.W. Lim, D.Y. Chung, M.J. Lee, H. Choe, Y.E. Sung, Ordered macroporous platinum electrode and enhanced mass transfer in fuel cells using inverse opal structure, Nat. Commun. 4 (2013) 1–9.

[29] N. Marquet, F. Gärtner, S. Losse, M.M. Pohl, H. Junge, M. Beller, Simple and efficient iridium(III)-catalyzed water oxidations, ChemSusChem. 4 (2011) 1598–1600.

[30] G.J.K. Acres, J.C. Frost, G.A. Hards, R.J. Potter, T.R. Ralph, D. Thompsett, G.T. Burstein, G.J. Hutchings, Electrocatalysts for fuel cells, Catal. Today. 38 (1997) 393–400.

[31] R.Q. Snurr, A.O. Yazaydin, A.I. Benin, S.A. Faheem, P. Jakubczak, J.J. Low, R.R. Willis, Enhanced CO(2) Adsorption in Metal-Organic Frameworks via Occupation of Open-Metal Sites by Coordinated Water Molecules, Chem. Mater. 21 (2009) 1425–1430.

[32] H.A. Mosqueda, C. Vazquez, P. Bosch, H. Pfeiffer, Chemical sorption of carbon dioxide (CO2) on lithium oxide (Li2O), Chem. Mater. 18 (2006) 2307–2310.

[33] M. Kato, S. Yoshikawa, K. Nakagawa, Carbon dioxide absorption by lithium orthosilicate in a wide range of temperature and carbon dioxide concentrations, J. Mater. Sci. Lett. 21 (2002) 485–487.

[34] S.R. Miller, G.M. Pearce, P.A. Wright, F. Bonino, S. Chavan, S. Bordiga, I. Margiolaki, N. Guillou, G. Férey, S. Bourrelly, P.L. Llewellyn, Structural transformations and adsorption of fuel-related gases of a structurally

responsive nickel phosphonate metal-organic framework, Ni-STA-12, J. Am. Chem. Soc. 130 (2008) 15967–15981.

[35] K.S. Walton, M.B. Abney, M.D. LeVan, CO2adsorption in y and X zeolites modified by alkali metal cation exchange, Microporous Mesoporous Mater. 91 (2006) 78–84.

[36] R. V. Siriwardane, M.S. Shen, E.P. Fisher, J.A. Poston, Adsorption of CO2on molecular sieves and activated carbon, Energy and Fuels. 15 (2001) 279–284.

[37] J. Lee, S.H. Yu, C. Kim, Y.E. Sung, J. Yoon, Highly selective lithium recovery from brine using a λ-MnO2-Ag battery, Phys. Chem. Chem. Phys. 15 (2013) 7690–7695.

[38] H. Yoon, J. Lee, S. Kim, J. Yoon, Review of concepts and applications of electrochemical ion separation (EIONS) process, Sep. Purif. Technol. 215 (2019) 190–207.

[39] T. Georgi-Maschler, B. Friedrich, R. Weyhe, H. Heegn, M. Rutz, Development of a recycling process for Li-ion batteries, J. Power Sources. 207 (2012) 173–182.

[40] J. Nan, D. Han, X. Zuo, Recovery of metal values from spent lithium-ion batteries with chemical deposition and solvent extraction, J. Power Sources. 152 (2005) 278–284.

[41] X. Zeng, J. Li, N. Singh, Recycling of spent lithium-ion battery: A critical review, Crit. Rev. Environ. Sci. Technol. 44 (2014) 1129–1165.

[42] F. Fu, Q. Wang, Removal of heavy metal ions from wastewaters: A review, J. Environ. Manage. 92 (2011) 407–418.

[43] H. Strathmann, Electrodialysis, a mature technology with a multitude of

new applications, Desalination. 264 (2010) 268–288.

[44] K.N. Mani, Electrodialysis water splitting technology, J. Memb. Sci. 58 (1991) 117–138.

[45] C. Charcosset, A review of membrane processes and renewable energies for desalination, Desalination. 245 (2009) 214–231.

[46] J. Lambert, M. Avila-Rodriguez, G. Durand, M. Rakib, Separation of sodium ions from trivalent chromium by electrodialysis using monovalent cation selective membranes, J. Memb. Sci. 280 (2006) 219–225.

[47] S.A. Kalogirou, Seawater desalination using renewable energy sources, Prog. Energy Combust. Sci. 31 (2005) 242–281.

[48] T. Hoshino, Development of technology for recovering lithium from seawater by electrodialysis using ionic liquid membrane, Fusion Eng. Des. 88 (2013) 2956–2959.

[49] T. Hoshino, Preliminary studies of lithium recovery technology from seawater by electrodialysis using ionic liquid membrane, Desalination. 317 (2013) 11–16.

[50] A.T. Cherif, J. Molenat, A. Elmidaoui, Nitric acid and sodium hydroxide generation by electrodialysis using bipolar membranes, J. Appl. Electrochem. 27 (1997) 1069–1074.

[51] M. Paleologou, A. Thibault, P.Y. Wong, R. Thompson, R.M. Berry, Enhancement of the current efficiency for sodium hydroxide production from sodium sulphate in a two-compartment bipolar membrane electrodialysis system, Sep. Purif. Technol. 11 (1997) 159–171.

[52] F. Alvarez, R. Alvarez, J. Coca, J. Sandeaux, R. Sandeaux, C. Gavach, Salicylic acid production by electrodialysis with bipolar membranes, J.

Memb. Sci. 123 (1997) 61–69.

[53] T. Xu, C. Huang, Electrodialysis-based separation technologies: A critical review, AIChE J. 54 (2008) 3147–3159.

[54] Y. Qu, T.F. Baumann, J.G. Santiago, M. Stadermann, Characterization of Resistances of a Capacitive Deionization System, Environ. Sci. Technol. 49 (2015) 9699–9706.

[55] P. Długołecki, P. Ogonowski, S.J. Metz, M. Saakes, K. Nijmeijer, M. Wessling, On the resistances of membrane, diffusion boundary layer and double layer in ion exchange membrane transport, J. Memb. Sci. 349 (2010) 369–379.

[56] A. Seidell, Solubilities of Inorganic and Organic Compounds., 2nd ed., van Nostrand Company, New York, 1952.

[57] V. Snoeyink, D. Jenkins, Water Chemistry, 1st ed., John Wiley & Sons, New York, 1980.

[58] Y. Zhou, H. Yan, X. Wang, L. Wu, Y. Wang, T. Xu, Electrodialytic concentrating lithium salt from primary resource, Desalination. 425 (2018) 30–36.

국 문 초 록

최근 실내 공기 질 개선에 관심이 증가하면서 실내 공기 중 CO_2 농도 제어를 위한 CO_2 흡착제 사용이 증가하고 있다. LiOH는 상온, 상압 조건에서 비교적 빠른 흡착 속도와 큰 CO_2 흡착용량으로 인해 CO_2 흡착 물질로 주목받고 있다. 하지만 최근 전기차, 배터리 시장이 급 발전함에 따라 리튬의 수요와 가치가 크게 증가함에도 불구하고, 사용이 완료된 리튬 기반의 CO_2 흡착제는 재활용, 재생산 되지 않고 버려지고 있었다.

따라서, 본 연구에서는 사용이 완료된 CO_2 흡착제에서 친환경적인 전기투석 방법을 사용하여 리튬을 회수하고 LiOH로 재생산하였다. Pt와 IrO_2 전극을 사용하여 전기화학적으로 각각 산소와 수소 발생 반응을 일으켜 리튬 이온이 수용액 내의 전기 중성도를 맞추기 위해 양이온 교환막을 통과하여 회수되는 시스템을 설계하였다. 사용된 CO_2 흡착제에서 전기화학적으로 LiOH를 생산하는 공정에서의 전류 운전 조건에 따른 리튬 회수 성능과 수용액 내의 이온들의 시간에 따른 전기화학적 거동을 분석하였다. 마지막으로 반복 운전을 통해 2.31M 의

LiOH로 농축하였고 결정화하여 분말형 LiOH를 생산하였으며 XRD와 SEM을 통해 결정구조를 분석하였다. 또한, 1g의 LiOH를 생산하기 위해 소모된 에너지를 분석하였다. 본 연구의 전류 조건에 따른 성능평가 및 에너지 소모량 분석 통해 전기화학적으로 흡착제를 재생하는 기술과 친환경 기술의 발전에 기여할 것으로 기대한다.

주요어: 전기화학적 리튬 회수, 전기 투석, 수산화 리튬, 이산화탄소 흡착제

학번: 2017-20743